Effects of Inhibitors on the Activity of the Cytochrome b_6f Complex: Evidence for the Existence of Two Binding Pockets in the Lumenal Site†

Romina Paola Barbagallo, Giovanni Finazzi,* and Giorgio Forti

Centro di Studio del CNR sulla Biologia Cellulare e Molecolare delle Piante, via Celoria 26, 20133 Milano, Italy

Received February 22, 1999; Revised Manuscript Received July 7, 1999

ABSTRACT: The effects of two inhibitors of electron transfer in the cytochrome b_6f complex have been studied in whole cells of *Chlamydomonas reinhardtii*. DNP-INT affected equally the two steps of the concerted oxidation of plastoquinol at the Q_o site; it decreased the rates of both cytochrome *f* reduction and cytochrome b_6 turnover, without affecting the amplitude of their redox signals. On the contrary, DBMIB inhibited only the rate of cytochrome *f* reduction while reducing, at the same time, the amplitude of cytochrome b_6 signals. The accessibility of DNP-INT to the Q_o site was unaffected by preillumination, while that of DBMIB was greatly enhanced, even after a single turnover of the cytochrome b_6f complex. Similar results were obtained with a mutant strain (FUD2) where the Q_o site has an affinity for plastoquinol that is diminished by a factor of ∼50 [Finazzi, G., et al. (1997) *Biochemistry 36*, 2867−2874]. However, the binding of the two inhibitors was differentially influenced by the mutation: a factor of ∼250 was calculated for DNP-INT and a factor of only ∼5 for DBMIB. This suggests that they bind within the Q_o site in two distinct pockets, which are differentially involved in the process of quinol oxidation, in agreement with a recent model where two distinct positions for the reduced and semireduced quinones are considered [Crofts, A. R., and Berry, E. A. (1998) *Curr. Opin. Struct. Biol. 8*, 501−509].

The cytochrome b_6f complex comprises four major subunits (*1*, *2*): the Rieske protein, which binds an Fe_2S_2 cluster, with an E_m of 290 mV (*3*); a *c*-type cytochrome, cytochrome *f*, with an E_m of 330 mV (*2*); a *b*-type cytochrome, cytochrome b_6, which binds the high- and low-potential hemes, b_h[1] and b_l, with E_ms of −84 and −158 mV, respectively (*2*); and subunit IV. In the green alga *Chlamydomonas reinhardtii*, three additional small subunits with unknown functions, the chloroplast *petG* and *petL* products and the nuclear product *PetM* (*2*, *4*), have been identified. Sequence comparisons have shown that cytochrome b_6 and subunit IV are homologous to the N- and C-terminal parts, respectively, of mitochondrial and bacterial cytochrome *b* (*5*). As a member of the *bc*-type proteins, the cytochrome b_6f complex couples proton translocation across the membrane to electron transfer from a lipophilic two-electron donor (plastoquinol) to a hydrophilic one-electron acceptor protein (plastocyanin or a *c*-type cytochrome). This electron transfer operates through a high-potential chain (also called the linear path) formed by the Rieske protein and cytochrome *f*.

In agreement with the "Q cycle" hypothesis of Mitchell (*6*), it has been shown that oxidation of quinols also involves a cyclic electron path around the *b* heme chain, termed the low-potential chain. The cycle, as modified by Crofts et al. (*7*), postulates both an oxidation and a reduction of the lipophilic electron carrier at two distinct sites of the protein, the Q_o and Q_i sites, on opposite sides of the membrane. The oxidation of plastoquinol at the Q_o site is associated with the reduction of both cytochrome *f* and b_l (*6*, *7*) and the release of protons into the lumen. Oxidation of the b_6 hemes occurs, instead, through a two-step reduction of a PQ molecule at the Q_i site. Thus, under oxidizing conditions, the electron-transfer sequence is a reduction by plastoquinol of cytochrome b_l which is in turn oxidized by cytochrome b_h. A second cytochrome b_6f turnover reduces both the b_l and b_h hemes, and causes the reduction of a plastoquinone to a plastoquinol at the Q_i site, *b* heme reoxidation, and proton uptake from the stromal space. Thus, the Q cycle results in extra proton translocation across the membrane, thereby increasing the H^+/e^- ratio of photosynthetic electron transfer.

The Q cycle provides the explanation for most of the experimental observations of the function of the cytochrome bc_1 or b_6f complex. However, this model does not provide a rationale for the operation of a branched quinol oxidation pathway (*8*, *9*). The thermodynamics of the system are such that a double-electron injection into the high-potential chain should be favored, at least under strong oxidizing conditions, where most of the electron acceptors in the high-potential

† This work was supported by the CNR (CNR Target Project on Biotechnology) and the CNR/CNRS exchange program (132.031, COM 04-14). R.P.B. was the recipient of a doctoral fellowship from the Ministero dell'Universita'e della Ricerca Scientifica e Tecnologica.

* Corresponding author. E-mail: finazzi@unimi.it. Telephone: 39 02 26604423. Fax: 39 02 26604399.

[1] Abbreviations: b_h, high-potential heme of cytochrome b_6; b_l, low-potential heme of cytochrome b_6; cyt, cytochrome; DBMIB, 2,5-dibromo-3-methyl-6-isopropyl-*p*-benzoquinone; DCMU, 3-(3′,4′-dichlorophenyl)-1,1-dimethylurea; DNP-INT, dinitrophenyl ether of iodonitrothymol; FCCP, carbonylcyanide *p*-(trifluoromethoxy)phenylhydrazone; HA, hydroxylamine; HEPES, *N*-(2-hydroxyethyl)piperazine-*N*′-2-ethanesulfonate; PC^+, oxidized plastocyanin; PC, reduced plastocyanin; PQ, plastoquinone; PQH_2, plastoquinol; PQ^-, plastosemiquinone; PS, photosystem; Q_i, quinol reducing site of the cytochrome b_6f complex; Q_o, quinol oxidizing site of the cytochrome b_6f complex.

10.1021/bi990424+ CCC: $18.00
Published on Web 09/09/1999

path are oxidized (*10*). Alternative models have been proposed, which partially overcome this problem. Among them, the *b*-type cycle of Wikstrom and Krab (*11*), as modified by Joliot and Joliot (*12*), proposes that the semiquinone molecule (PQ^-), which is generated by the electron transfer to the cytochrome *f*, is translocated through the membrane from the Q_o site to the Q_i site where it is reduced by an electron that is transferred from the b_h heme. This movement would prevent the transfer of a second electron to the Rieske protein. At variance with the Q cycle, where electron transfer can be initiated only if one of the *b* hemes is oxidized, the semiquinone cycle takes place also when the *b* hemes are fully reduced. In support of the semiquinone cycle hypothesis, cytochrome b_6f-dependent charge translocation across the membrane was observed even when the b_6 cytochromes were completely reduced (*12*, *13*). To explain this observation within the frame of the Q cycle, a "reaction chain" mechanism, where oxidation of the b_6 hemes occurs through multiple turnovers of the cytochrome b_6f complex, has been proposed by Kramer and Crofts (*14*).

A third model exists, which has been proposed by Joliot and Joliot to explain the effect of inhibitors of the Q_i site (*15*). It postulated the existence of a "double-pocket Q_o site", and a quinol movement between the two pockets during its oxidation. Later, Ding and co-workers (*16*, and references therein) proposed independently a rather similar situation, where the two pockets are occupied at the same time by two quinols. In their model, Ding and co-workers propose that the consecutive transfer of two electrons into the high-potential chain is prevented by the simultaneous oxidation of the quinols to a semiquinone state during a turnover, and their consecutive disproportionation (*16*). The same conclusion has also been reached by Brandt to explain the noncompetitive inhibition of some quinol analogues on isolated mitochondrial bc_1 complexes (*17*).

Recently, the structure of the respiratory bc_1 complex has been determined by X-ray crystallography in several laboratories (*18*−*20*). It has been reported that the soluble domain of the Rieske protein assumes different conformations with respect to its membrane part (*19*−*22*). A movement of the quinol molecule has also been predicted, on the basis of the position within the Q_o site of residues responsible for the resistance to different inhibitors (*19*−*21*). An interpretative model has been then proposed (*19*, *20*, *23*), according to which the quinol and the oxidized Rieske protein stay close together in the Q_o site until an electron is transferred to the iron, when they move apart to reduce the b_l and *c* hemes, respectively. Thus, the concerted movement of the Rieske protein and of the semiquinone prevents the transfer of two electrons to the high-potential chain.

To test whether the same or a similar mechanism is operating in the cytochrome b_6f complex, we have performed experiments in *C. reinhardtii* cells, to study the effect of inhibitors of the Q_o site on the electron injection into the linear and cyclic paths in a fully native system. We show that uncoupling of cyclic electron flow from the linear path is observed when one of the inhibitors is used, DBMIB. This confirms the existence of two quinone binding pockets also in the Q_o site of the photosynthetic cytochrome complex. In addition, we show that the DBMIB site is accessible only after one turnover has occurred, which is consistent with the mechanism described above, where the movement of the Rieske protein is predicted to modify the accessibility to the inner part of the Q_o site.

MATERIALS AND METHODS

C. reinhardtii wild-type cells, derived from strain 137C, and the mutant FUD2, where the affinity for PQH_2 is greatly diminished (*24*), were kindly provided by the Laboratoire de Physiologie Membranaire et Moléculaire du Chloroplaste at the Institut de Biologie Physico Chimique of Paris (France). Cells were grown at 27 °C in acetate-supplemented medium (*25*) under ∼60 μE m^{-2} s^{-1} of continuous white light. They were harvested during the exponential growth phase and resuspended at the required concentration in a 30 mM HEPES medium (pH 7.2) with 10% (w/v) Ficoll, to avoid sedimentation. DBMIB was purchased from Sigma, while DNP-INT was a kind gift from W. Oettmeier and A. Trebst (Bochum, Germany).

Spectroscopic measurements were performed at room temperature, using a "Joliot type spectrophotometer" as described by Joliot et al. (*26*). Actinic flashes were provided by a xenon lamp (3 μs at half-height) filtered through a Schott filter (RG 695). They were fired at a frequency of 0.15 Hz and were nonsaturating (hitting ∼25% of the centers) unless otherwise indicated. Algae were kept in the dark under an argon atmosphere in a large reservoir, connected to the measuring cuvette, to ensure dark reduction of the PQ pool.

The transmembrane potential was estimated with the amplitude of the electrochromic shift at 515 nm, which yields a linear response with respect to the electric component of the transmembrane potential (*27*). Under the conditions employed here, the kinetics of the electrochromic signal exhibited two phases previously described in ref *28*: a fast phase completed in less than 1 μs, associated with PS1 and PS2 charge separation (phase a), and a slow phase which develops in the millisecond time range, associated with the turnover of the cytochrome b_6f complex (phase b). PS2 absorption changes were prevented by a preillumination in the presence of DCMU (10 μM) and HA (1 mM) (*29*). Thus, phase a was indicative of the sole PS1 charge separation.

The kinetics of phase b were deconvoluted from membrane potential decay, assuming that the latter process exhibited first-order kinetics. Phase b was then computed considering that the rate of membrane potential decay was linearly related to its actual value. A deconvolution of phase b kinetics assuming multiexponential kinetic decays for membrane potential did not improve significantly the results of the procedure (not shown). This is not surprising since phase b proceeds in the 5−10 ms time range, whereas the transmembrane potential decay exhibits two phases with half-times in the hundreds of milliseconds and in the seconds time ranges (*28*). Therefore, only the fastest one is expected to superimpose with the b phase kinetics.

Cytochrome *f* redox changes were evaluated as the difference between absorption at 554 nm and a baseline drawn between 545 and 573 nm. A small correction for the contribution of the electrochromic signal (5% of the signal observed at 515 nm) was made. Cytochrome b_6 redox changes were measured as the difference between the absorption at 564 nm and the same baseline.

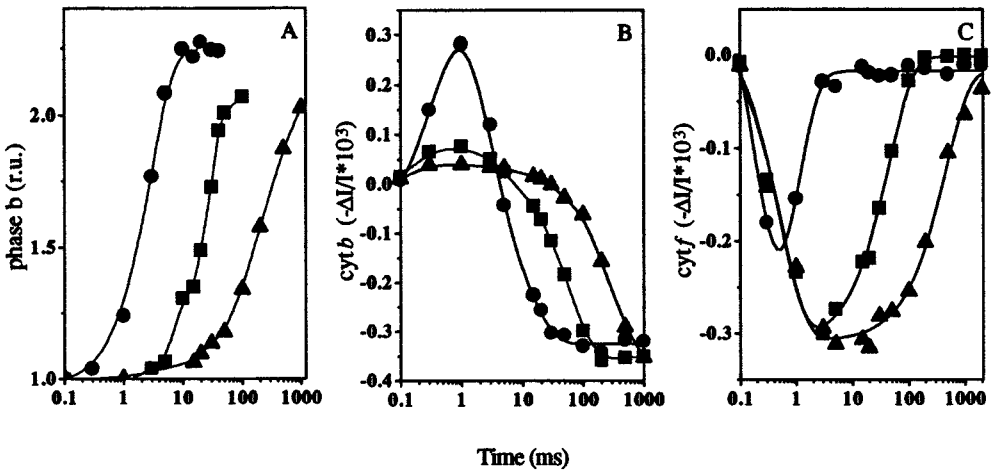

FIGURE 1: Influence of DNP-INT on the kinetics of the slow electrochromic signal (phase b) (A), cytochrome b_6 (B), and cytochrome *f* (C) redox changes. Algae were illuminated with nonsaturating red flashes (hitting ~25% of the centers) at a frequency of 0.15 Hz in 20 mM HEPES (pH 7.2) and 10% Ficoll. DCMU and HA were added at concentrations of 10 μM and 1 mM, respectively, to block PS2 activity. The kinetics of the slow electrochromic signal were corrected for the membrane potential decay as described in Materials and Methods. All measurements were performed in the presence of 1 μM FCCP to collapse the electrochemical proton gradient existing in the dark: (●) no addition, (■) 1 μM DNP-INT, and (▲) 10 μM DNP-INT. The chlorophyll concentration was 70 μM.

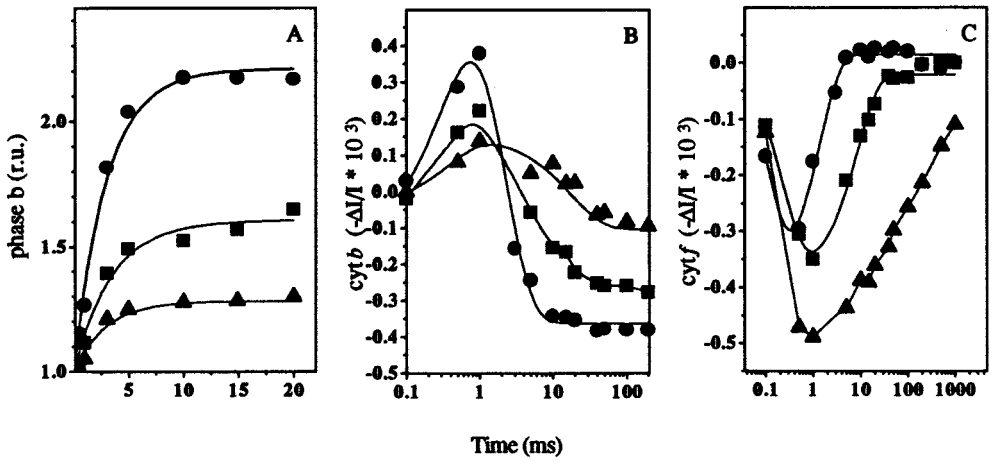

FIGURE 2: Influence of DBMIB on the kinetics of the slow electrochromic signal (A), cytochrome b_6 (B), and cytochrome *f* (C) redox changes. Note the use of a linear time scale in the case of panel A: (●) no additions, (■) 20 μM DBMIB, and (▲) 35 μM DBMIB. Other conditions were as described in the legend of Figure 1.

RESULTS

Effects of Q_o Site Inhibitors on Cytochrome b_6f Activity. Figure 1 shows the effects of increasing concentrations of DNP-INT on the kinetics of phase b (A), cytochrome b_6 (B), and cytochrome *f* (C) turnover, which reflect the rate of PQH_2 oxidation in the Q_o site of the cytochrome b_6f complex (see refs *8*, *9*, and *30*). In Figure 1A, PS2 activity was inhibited through the addition of DCMU and HA to the cells. Thus, the kinetics of phase b are presented after normalization to the amplitude of PS1-driven phase a. The addition of HA and DCMU blocked the light generation of plastoquinol by PS2. Nevertheless, the PQ pool was fully reduced in the dark by cellular metabolism (*12*), and the cytochrome b_6f Q_o site was consequently saturated (see ref *24*). We checked, by measuring fluorescence emission, that the redox state of the PQ pool was unaffected by the different treatments reported below (not shown).

In panels B and C of Figure 1, the reduction phases of the cytochrome redox changes are shown as upward changes, whereas oxidation phases are shown as downward changes.

DNP-INT is a quinone analogue known to be a competitive inhibitor of the plastoquinol oxidation at the Q_o site of cytochrome b_6f (*31*). Thus, as expected, it inhibited at the same time the rates of phase b and cytochrome *f* reduction. The $t_{1/2}$ of the reactions changed from ~2 ms in the absence of the inhibitor to ~200 ms when the inhibitor was added at a concentration of 10 μM. Both the reduction and oxidation rates of cytochrome b_6 were similarly affected. The specificity of DNP-INT as an inhibitor of the Q_o site was proven by the observation that it had little effect (if any) on the rate of cytochrome *f* oxidation (Figure 1C), which depends only on the electron transfer between cytochrome *f* and plastocyanin (*8*, *9*). Similar results were obtained when another inhibitor of the Q_o site, stigmatellin, was added to the cells of *Chlamydomonas* (not shown).

When another commonly used quinone inhibitor, DBMIB (see refs *32* and *33*), was added to the cells, the rate of cytochrome *f* reduction was decreased from 2 to ~150 ms at 35 μM DBMIB (Figure 2C). On the contrary, the rates of both the phase b and cytochrome b_6 turnover were slightly affected even when DBMIB was added at a concentration

of 30−40 μM. Their amplitudes, but not that of cytochrome *f*, were diminished (compare panels A and B with panel C of Figure 2) by DBMIB. The effect on the rate of cytochrome *f* reduction and on the amplitude of the phase b and the cytochrome b_6 signal showed a similar concentration dependence, suggesting a close relationship between these phenomena. Electron transfer through cytochrome *f* could be fully inhibited by DBMIB at high concentrations. At lower DBMIB concentrations, DNP-INT addition blocked completely the kinetics of cytochrome *f* reduction (not shown). This indicates that DBMIB was unable to reduce directly the cytochrome *f* heme, even at the high concentrations employed here, at variance with previous reports (*34*, *35*) where stigmatellin insensitive electron donation to cytochrome *f* was observed at high DBMIB concentrations. As in the case of DNP-INT, the effect of DBMIB was specific for the Q_o site; the rate of cytochrome *f* oxidation was unaffected by its addition (Figure 2C).

The results depicted in Figures 1 and 2 refer to measurements performed with nonsaturating flashes under repetitive conditions; i.e., they represent the average of several single-flash illuminations (from 10 to 20). In the case of DNP-INT, we observed the same inhibition irrespective of the number of illuminations. In the case of DBMIB, on the contrary, several turnovers were required before the amplitude of phase b (or of cytochrome b_6 redox changes) was reduced to its minimum (not shown). Increasing the illumination frequency reduced the concentration of DBMIB required to obtain the maximal inhibitory effect to ~5 μM (not shown). This value is still higher than that usually employed in vitro, but in the same range as in previous works with intact cells (*36*−*38*). This suggests that both the inhibitor concentration and the illumination frequency contribute synergistically to the inhibition of cytochrome b_6f complexes by DBMIB. The data depicted in Figure 2 did not allow estimation of the number of catalytic cycles required to observe the maximal effect of DBMIB because only a small fraction of cytochrome b_6f complexes performed a turnover at each illumination under subsaturating flash regimes. Thus, we repeated the same experiment at saturating intensity, a condition where all the cytochrome b_6f complexes perform a turnover during each illumination. In these experiments, saturating concentrations of DBMIB (Figure 3A,B) were also employed to ensure that all the cytochrome b_6f complexes had bound DBMIB in the dark. Under these conditions, we observed (Figure 3A) that a single preillumination was sufficient to increase the effect of DBMIB close to its maximum extent, in agreement with previous observations by Rich et al. (*34*) with isolated spinach thylakoids. The rate of cytochrome *f* reduction remained unaffected after the first illumination and was only slightly decreased after the second (not shown).

After illumination, a recovery of the amplitude of phase b could be observed, provided that the cells were left long enough in the dark (Figure 3A). We have measured the time required to recover from inhibition, after a sequence of flashes fired 4 s apart, and we have calculated a $t_{1/2}$ in the 10 s range (Figure 3C).

Effects of Q_o Site Inhibitors on FUD2 Mutant Cells. The effects of DNP-INT and DBMIB on the kinetics of the cytochrome b_6f complex (Figures 1 and 2), together with the finding that DBMIB, but not DNP-INT, requires a preillumination to cause inhibition at the Q_o site (Figure 3), suggest either that the two inhibitors affect different steps of the oxidation of PQH_2 or that they bind in different loci of the Q_o site. Clearly, the two hypotheses are not mutually exclusive. To discriminate between these possibilities, we have studied the effect of both inhibitors on the activity of the cytochrome b_6f complex in FUD2 cells. The Q_o site of this mutant is greatly perturbed by a duplication of 12 amino acids within the cd2 loop of the cytochrome b_6 moiety that reduces the affinity for PQH_2 by a factor of ~50 (*24*). Thus, we expected different responses to DNP-INT and to DBMIB in FUD2, if they bound at different loci of the Q_o site.

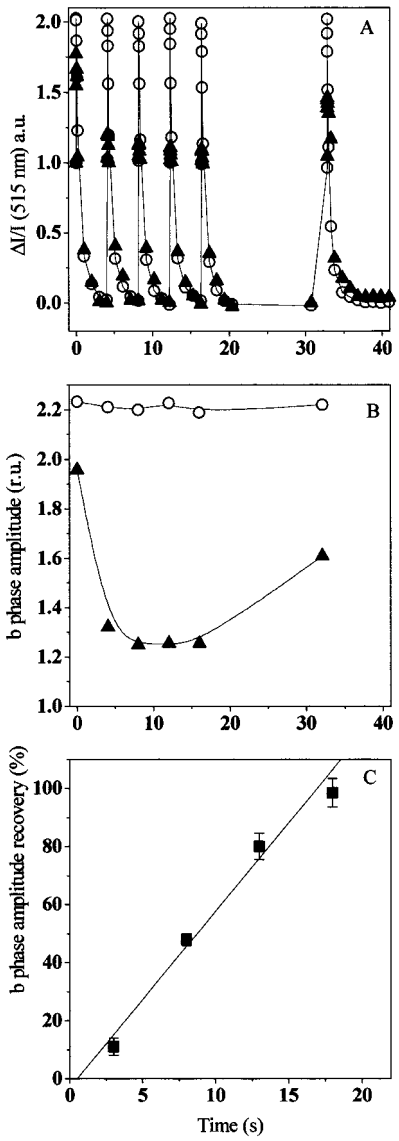

FIGURE 3: (A) Effects of DBMIB on the magnitude of the slow electrochromic signal after illumination with a series of saturating single-turnover flashes. Saturating flashes were fired at a frequency of 0.25 Hz: white symbols, no additions; and black symbols, 20 μM DBMIB. (B) Estimation of the amplitude of phase b upon illumination with saturating single-turnover flashes. The phase b amplitude was deconvoluted as explained in Materials and Methods. (C) Kinetics of recovery from inhibition by DBMIB in the dark. The kinetics have been measured varying the time between two consecutive illuminations after a sequence of four flashes. Figures represent the average from three different experiments.

In FUD2, we obtained qualitatively the same results as in the wild-type strain upon addition of DNP-INT and DBMIB; the former decreased the rate of all PQH_2 oxidation steps,

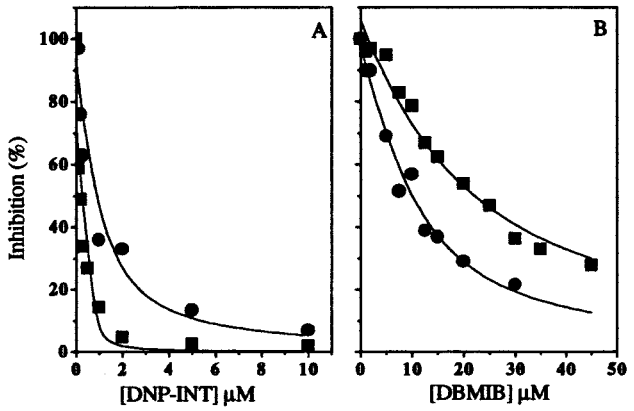

FIGURE 4: Relationship between the inhibition of the slow electrochromic signal and the amount of added DBMIB and DNP-INT in wild-type (■) and FUD2 cells (●) of *C. reinhardtii.* The same conditions that are described in the legend of Figure 1 were used. Inhibition refers to the magnitude of the slow electrochromic signal in panel A and to the slowing of the signal kinetics in panel B.

while the latter affected only the rate of cytochrome *f* reduction, decreasing at the same time the amplitudes of both the phase b and the cytochrome b_6 redox signals (not shown). However, the concentration dependence of the DNP-INT and DBMIB effects was significantly different in wild-type and FUD2 cells (Figure 4); the mutant was less sensitive to DNP-INT (panel A) than the wild type but more sensitive to DBMIB (panel B).

From the curves reported in Figure 4, we have estimated the apparent dissociation constant for the inhibitors, using the following relation (*39*, *40*):

$$\%\ \text{inhibition} = \frac{1}{2[\text{E}]}[[\text{E}] - K_{\text{D,app}} - [\text{I}] + \sqrt{([\text{I}] + K_{\text{D,app}} - [\text{E}])^2 + 4K_{\text{D,app}}[\text{E}]}] \quad (1)$$

which expresses the extent of inhibition in terms of the concentration of the cytochrome b_6f complex ([E]), that of the inhibitors ([I]), and the apparent dissociation constant for the inhibitor that is used ($K_{\text{D,app}}$).

The results are reported in Table 1. We observed that the values calculated for both the dissociation constants and the enzyme concentrations were remarkably higher than previously reported in vitro (*39*). This overestimation may arise from two experimental difficulties which might occur under our conditions. First of all, the concomitant binding and unbinding of DBMIB at rather low frequencies of illumination might result in a decreased efficiency of the inhibitor, as a consequence of the use of nonsaturating flashes. In this case, the utilization of eq 1, which applies only in the case of tight binding inhibitors (*40*), would not be correct. Two points, however, do not support this possibility. First of all, the calculated ratio between the concentration of the enzyme and the K_D reported here for DBMIB is very similar to that previously reported in isolated systems in the case of DBMIB (*34*, *39*). This demonstrates that the inhibitor behaves as a tight binding one under our experimental conditions, and that the utilization of eq 1 is correct. Moreover, the same enzyme concentration was calculated from both the DBMIB and DNP-INT concentration curves (Table 1). The binding of this latter inhibitor, however, is not affected by the illumination frequency or by the flash intensity (Figure 3); i.e., it is not subject to the same binding and unbinding properties as DBMIB.

Thus, we conclude that the binding properties of DBMIB are not the main cause of the discrepancy between the parameters reported here and in previous in vitro work (*34*, *39*). Rather, we attribute this discrepancy to an overestimation of the inhibitors concentration, which would stem from their dilution in the different cellular compartments and other membranes, a phenomenon previously observed with other quinone analogues (*41*). This dilution would reduce the true inhibitor concentrations in the thylakoid membrane, the estimation of which would require the knowledge of their partition coefficients, which are not known. However, we do not expect differences in the partition coefficients for DBMIB and DNP-INT between the wild-type and FUD2 cells, which differ only in the structure of the Q_o site of the cytochrome b_6f complex. Thus, we performed an analysis in terms of the sole comparison between the wild-type and FUD2 strains.

We observed that the cytochrome b_6f complex concentration calculated from the fit was very similar in the wild-type and FUD2 cells. This confirms the validity of this comparative approach, since the cytochrome b_6f concentration is indeed very similar in both strains, on a chlorophyll basis (*24*). From the figures calculated above, we have estimated the true dissociation constants, using the K_D values calculated by Finazzi and colleagues for both the mutant and the wild-type cytochrome b_6f complexes (*24*) and the PQH_2 concentration given in ref *42*. The results are reported in Table 1. Again, we performed only a comparative analysis of the results, since we are aware that the calculated values are susceptible to the same overestimation discussed above. The results revealed a marked effect of the mutation on the affinities; while FUD2 had a K_D for plastoquinol that was 50 times higher than that of the wild type (*24*), the ratio increased to 250 in the case of DNP-INT, and decreased to only 5 in the case of DBMIB. This difference between the mutant and wild-type cytochromes strongly suggests that the two inhibitors bind to different sites.

Table 1: Dissociation Constants for the Q_o Site for Plastoquinol, DNP-INT, and DBMIB in the Cytochrome b_6f Complex of Wild-Type and FUD2 Cells of *C. reinhardtii*[a]

		PQH_2	DBMIB		DNP-INT	
	[E] (M)	K_D (M)	$K_{D,app}$ (M)	K_D (M)	$K_{D,app}$ (M)	K_D (M)
wild-type	9.4×10^{-6}	5×10^{-5}	1.5×10^{-5}	7×10^{-7}	3.2×10^{-8}	1.4×10^{-9}
FUD2	9.7×10^{-6}	2×10^{-3}	5.4×10^{-6}	3.6×10^{-6}	5.5×10^{-7}	3.7×10^{-7}

[a] Values are calculated from least-squares fitting of the data depicted in Figure 4, using eq 1 as explained in the text. [E] represents the concentration of the cytochrome b_6f complex. Essentially the same values of [E] were calculated from the traces relative to DBMIB or DNP-INT inhibition.

DISCUSSION

Effects of DNP-INT and DBMIB on Cytochrome b_6f Activity. Our results confirm that DNP-INT and DBMIB behave as Q_o site inhibitors in vivo. Their mechanism of action is nevertheless different. DNP-INT behaves as a classical competitive inhibitor; it decreases the rates of all reactions that follow PQH_2 oxidation, along the high-potential (Figure 1C) and the low-potential chain (Figure 1A,B). The rationale for this would be that the inhibitor inactivates a fraction of the complexes, and those left have to turn over several times to reduce all the positive charges (PC^+) generated by PS1 photochemistry. This explanation has already been proposed in the case of other photosynthetic systems (*43*).

In Figure 1B, we report that both the reduction and oxidation of cytochrome b_6 are inhibited by DNP-INT. This is expected since the oxidation of b_6 hemes takes place only after the b_l heme has been reduced, according to the following sequence of events: reduction of b_l by PQ^- (which corresponds to the small upward signal in Figure 1B) and oxidation of b_l by b_h, which occurs after the electron transfer from b_h to a quinone molecule at the Q_i site. This latter process contributes to the large downward signal in Figure 1B. This figure shows that the rates of these three reaction steps are comparable, in agreement with the notion that the turnover of cytochrome b_6 is governed by the overall equilibrium between the PQ^-, b_l, and b_h hemes (reviewed in refs *8* and *9*). Thus, it is conceivable that the decreased kinetics of cytochrome b_6 oxidation measured in the presence of DNP-INT simply arise from the inhibition of electron transfer from PQ^- to b_l.

The effects of DBMIB are more complex. On one hand, its decreasing cytochrome *f* reduction kinetics, without changing the signal amplitude (Figure 2C), reproduces that of DNP-INT, again providing evidence for the occurrence of multiple turnovers along the high-potential chain of the noninhibited cyt b_6f complexes. On the other hand, the decreased amplitude of both phase b and cytochrome b_6 signals, the kinetics of which were substantially unaffected by DBMIB (Figure 2A,B), is evidence that only one turnover is possible along the low-potential chain when DBMIB is bound.

Therefore, the main difference between the DBMIB and DNP-INT effects on cytochrome b_6f turnover is at the level of the electron donation to the low-potential chain; the PQH_2 oxidation is still concerted in the presence of DNP-INT, while it is not in the presence of DBMIB.

Investigating the effect of DNP-INT on cytochrome b_6f kinetics, Delosme et al. (*31*) observed that the kinetics of electron transfer were always monophasic even upon addition of DNP-INT. These authors interpreted it as a consequence of the very fast exchanging rate of DNP-INT (higher than 100 s^{-1}). However, monophasic kinetics have also been reported in the case of DBMIB (*32*, *34*), the dissociation rate of which is very slow (*34*; Figure 3). Rich and colleagues (*34*) attributed the lack of biphasicity to the very rapid inter-*bf* equilibrating rates of plastocyanin, which are at least 1 order of magnitude faster than those of cytochrome b_6f complex turnover. Our results are fully consistent with this latter hypothesis, which had already been discussed by Haehnel (*44*).

DBMIB Binding Site in the Cytochrome b_6f Complex. The different effects of DNP-INT and DBMIB on the activity of cytochrome b_6f complex can be easily understood in terms of the different binding of the two inhibitors within the Q_o site; while DNP-INT would compete with PQH_2, DBMIB would occupy a separate "pocket" in the Q_o site, where it would block only the electron transfer to the b_l heme. Two experimental observations support this possibility: (i) the increased accessibility of the inhibitor to the Q_o site after a single turnover of cytochrome b_6f complexes and (ii) the differential effect of the FUD2 mutation on the dissociation constant of DNP-INT, PQH_2, and DBMIB.

The changes in the affinity of the Q_o for DBMIB upon illumination are clearly illustrated by the data reported in Figure 3. In these experiments, the amplitude of phase b is measured to probe the amount of active cytochrome b_6f complexes, i.e., those that did not bind DBMIB in the dark. Thus, the decrease in the phase b amplitude from ~0.7 (before illumination) to ~0.2 (after the first flash) (Figure 3A,B) is indicative of an increased level of binding of DBMIB, i.e., of an enhanced accessibility of the inhibitor to the cytochromes, as a consequence of their catalytic cycle.

In the cytochrome bc_1 complex, it has been documented that the binding sites for myxothiazol and stigmatellin are not identical, the first being located closer to the b_l heme than the latter (*19*−*21*). This finding has suggested a model where the semiquinone moves from the stigmatellin to the myxothiazol site and reduces the b_l heme, after the first electron has been transferred to the Rieske protein from ubiquinol (*20*, *21*, *23*). In the bc_1 structure, the quinol pocket is close to the Q_o site entrance, while the other (the semiquinone one) is located deeper in the membrane (*19*−*21*). The two pockets are not identically accessible, the overall accessibility of the semiquinone site being controlled by the movements of the Rieske protein (*20*), which allows the release of the oxidized quinone from the catalytic site. If this situation is transposed to the case of the cytochrome b_6f complex, then the increased level of inhibition by DBMIB upon illumination can be explained in terms of its binding to the semiquinone site, where it would have access after the catalytic cycle of the complex, when PQ is released. On the contrary, DNP-INT would bind directly to the quinol pocket and would therefore be insensitive to preillumination.

The effect of the FUD2 mutation, where the binding of DNP-INT is more affected than that of DBMIB, is consistent with this hypothesis. As already stated, the calculation of the true dissociation constants for the inhibitors is affected by the uncertainty of their real concentration, because of membrane dilution of the inhibitors. Nevertheless, the comparative analysis of the inhibitor sensitivity of the wild-type and mutant strains clearly indicated that the inhibitor efficiency is strongly and selectively perturbed in the FUD2 Q_o site. Since the degree of homology between the Q_o sites of *bc* and *bf* complexes is very high (*35*), it is justified to resort to the X-ray structure of the bc_1 complex. In this structure, the cd2 loop is closer to the quinol site than to the putative semiquinone one (*19*−*21*, *23*), which should then be less affected by the structural modifications induced by the mutation, as we observed (Table 1). On the contrary, the effects of the mutation on the DNP-INT dissociation constant suggest that it probably binds closer to the cd2 loop than the plastoquinol itself.

Origin of the Electron-Transfer Reactions in DBMIB-Treated Cytochrome b_6f Complexes. As stated above, the electron donation to cytochrome *f* and b_6 is no more concerted in the presence of DBMIB; the turnover of the b_6 hemes occurs only in a fraction of active complexes, and is completed after a single catalytic cycle, while the reduction of cytochrome *f* involves the totality of the active cytochromes, and requires multiple turnovers. Thus, a fraction of the cytochromes b_6f exists, where reduction of cytochrome *f* but not of cytochrome b_l occurs. This possibility is fully consistent with very recent EPR data, which have demonstrated the binding of DBMIB to the Q_o site, in a position very close to the b_l heme pocket (*45*).

This population of cytochrome b_6f complexes, therefore, should contain either a PQH_2 that cannot transfer electrons to the low-potential chain because of the simultaneous presence of DBMIB or an electron donor that is not the physiological one, such as DBMIB in its reduced form (*46*).

The first hypothesis predicts that DBMIB inhibits electron transfer to the b_l heme, by competing with PQ^- for its binding site. This situation is reminiscent of that reported by Brandt (*17*) in the case of the mitochondrial bc_1 system, where E−β-methoxyacrylates affect the electron-transfer activity via noncompetitive binding to the cytochrome bc_1 complex. However, DBMIB would still behave as a competitive inhibitor of the overall concerted PQH_2 oxidation at the Q_o site, in agreement with the findings of Nanba and Katoh (*47*), because of its competition with the semiquinone for its binding pocket.

On the contrary, we consider the second hypothesis rather unlikely, since our evidence that the binding sites for PQH_2 and DBMIB are not the same does not support the occurrence of an efficient electron transfer by DBMIB. The distance between DBMIB in the semiquinone pocket and the Rieske protein is, indeed, too large (*20*, *21*, *23*) to account for electron transfer in the millisecond time range (*48*). Nevertheless, we cannot rule out the possibility that the reduced form of DBMIB ($DBMIBH_2$) might bind in the Q_o site closer to the quinol pocket, where it would donate electrons to the Rieske FeS center before moving to its inhibitory site. Thus, $DBMIBH_2$ would mimic the movements of plastoquinol, and would reduce the Rieske FeS center even in the absence of bound PQH_2 (*46*).

To summarize the behavior of cytochrome b_6f in the presence of DBMIB in the frame of these two hypothesis, we propose a hypothetical model (Scheme 1) where the existence of several populations of the complex is postulated. According to the first one, four of them (representing the different combinations of a substrate and an inhibitor binding simultaneously to an enzyme) are in equilibrium, while the fifth one is a dead-end inhibited state (see above). On the contrary, in the frame of the second hypothesis, DBMIB behaves at the same time as the substrate and the inhibitor. Thus, the number of states is reduced to four, the ESI and EI populations being identical (complexes bound to $DBMIBH_2$), while the predicted kinetic behavior is essentially the same.

Cytochrome b_6f complexes containing a PQH_2 molecule (ES) would transfer electrons to both the linear (high-potential) and the cyclic (low-potential) paths, while ESI centers (or ESI and EI, according to the second hypothesis) would only reduce cytochrome *f*. Thus, the phase b signal would be generated only by the ES population. Before illumination, K_{DI} would be comparable to K_{DS}[2] and most of the complexes would be in the ES state (Figure 3A,B, first flash) because of the high concentration of PQH_2 in the membranes (*42*). After a flash, the affinity for DBMIB would increase, because of the decreased K_{DI}, and the EI and ESI states would prevail over ES (Figures 2 and 3A,B).

A simple calculation[2] indicates that after the first flash only ~5% of the complexes remain in the ES state in the presence of 10 μM DBMIB, while only 2% is obtained with 30 μM. The transformation of ES centers into ESI (and eventually EX) after one single catalytic act would prevent multiple turnovers of the ES centers. On the contrary, the accumulation of EX, which is inactive, would be responsible for the occurrence of multiple turnovers in the remaining active centers, i.e., the ESI (or the sum of ESI and EI, according to the second hypothesis) population. This would

Scheme 1: Hypothetical Mechanism for Cytochrome b_6f Turnover in the Presence of DBMIB[a]

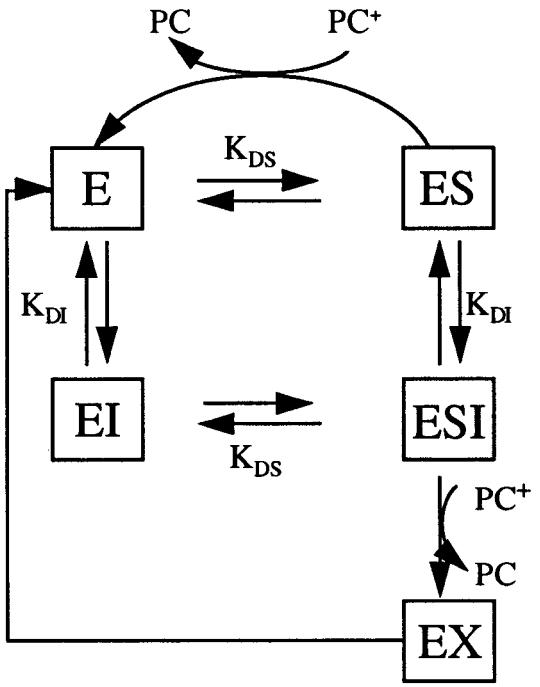

[a] E, ES, EI, and ESI stand for cytochrome b_6f complexes devoid of ligands and bound to PQH_2, DBMIB, or both PQH_2 and DBMIB, respectively. EX stands for dead-end inhibited cytochrome b_6f complexes. K_{DS} and K_{DI} are the dissociation constants for PQH_2 and DBMIB, respectively. Electron-transfer competent reactions in cytochrome b_6f complexes are described as the reduction of plastocyanin (PC^+ to PC). See the text for further details

[2] We consider that, before the first catalytic cycle of the cytochrome b_6f complex, the ratio between the PQH_2-bound complexes (ES) and those bound to DBMIB (EI + ESI) is equal to $[K_{DI}/(K_{DS} + [S])][[S]/[I])$, where K_{DS} and K_{DI} are the dissociation constants for the plastoquinol (S) and DBMIB (I), respectively, and [S] and [I] are their concentrations, respectively. Among these parameters, K_{DS}, [I], and [S] are not expected to vary before and after a turnover of the cytochrome b_6f complex. Thus, we may use their values reported in Table 1 and a ES/(EI + ESI) ratio of 0.7/0.3 (Figure 3A) to calculate a K_{DI} of 7.35 $\times$ 10^{-5} M before illumination. This value is to compare with that estimated after illumination (7×10^{-7} M; see Table 1). Using the same values, the dark distribution of each state can be calculated according to the following equations: $ES/E_{tot} = [S]K_{DI}/(K_{DS} + [S])(K_{DI} + [I])$; $EI/E_{tot} = [I]K_{DS}/(K_{DS} + [S])(K_{DI} + [I])$; $ESI/E_{tot} = [S][I]/(K_{DS} + [S])(K_{DI} + [I])$; $E/E_{tot} = K_{DS}K_{DI}/(K_{DS} + [S])(K_{DI} + [I])$.

decrease progressively the rate of cytochrome *f* reduction, essentially by the same mechanism operating in the presence of DNP-INT (see above). Free cytochrome b_6f complexes (E) would be slowly regenerated ($t_{1/2} \sim 10$ s) (Figure 3C) by the dark reduction of the EX states at the expense of the cellular reducing power, as previously reported in the case of both the b_6 and the *f* hemes (*49*, *50*). This slow conversion would regenerate active complexes that would account for the cytochrome b_6f activity observed under steady-state conditions (Figure 2). The regeneration would be affected by the illumination frequency, which would modulate the EX/E ratio, and/or by the concentration of DBMIB, which would shift the equilibrium toward EI at the expense of ES. Both these effects would account for the observed synergy of the inhibitor concentration and the illumination frequency in the effect on the efficiency of DBMIB as an inhibitor.

ACKNOWLEDGMENT

The authors are grateful to Prof. Pierre Joliot (Paris, France) for his criticism and contribution during the first phase of this work. Thanks are also due to Stefano Santabarbara (Milan, Italy), Frauke Baymann, Fabrice Rappaport, and Francis André Wollman (Paris, France), and Cécile Breyton (Frankfurt, Germany) for critical discussions and to Prof. Carlo Soave (Milan, Italy) for his criticism and suggestions upon reading the manuscript.

REFERENCES

1. Lemaire, C., Girard-Bascou, J., Wollman, F., and Bennoun, P. (1986) *Biochim. Biophys. Acta 851*, 229−238.
2. Pierre, Y., Breyton, C., Kramer, D., and Popot, J. (1995) *J. Biol. Chem. 49*, 29342−29349.
3. Nitschke, W., Joliot, P., Liebl, U., Rutherford, A. W., Hauska, G., Müller, A., and Riedel, A. (1992) *Biochim. Biophys. Acta 1102*, 266−268.
4. Takahashi, Y., Rahire, M., Breyton, C., Popot, J.-L., Joliot, P., and Rochaix, J.-D. (1996) *EMBO J. 15*, 3498−3506.
5. Widger, W. R., Cramer, W. A., Herrmann, R. G., and Trebst A. (1984) *Proc. Natl. Acad. Sci. U.S.A. 81*, 674−678.
6. Mitchell, P. (1975) *FEBS Lett. 56*, 1−6.
7. Crofts, A. R., Meinhardt, S. W., Jones, K. R., and Snozzi, M. (1983) *Biochim. Biophys. Acta 723*, 202−218.
8. Hope, A. B. (1993) *Biochim. Biophys. Acta 1143*, 1−22.
9. Cramer, W. A., Soriano, G. M., Ponomarev, M., Huang, D., Zhang, H., Martinez, S. E., and Smith, J. L. (1996) *Annu. Rev. Plant Physiol. Plant Mol. Biol. 47*, 477−508.
10. Brandt, U. (1996) *Biochim. Biophys. Acta 1275*, 41−46.
11. Wikstrom, M., and Krab, K. (1986) *J. Bioenerg. Biomembr. 18*, 181−193.
12. Joliot, P., and Joliot, A. (1994) *Proc. Natl. Acad. Sci. U.S.A. 91*, 1034−1038.
13. Moss, D. A., and Rich, P. R. (1987) *Biochim. Biophys. Acta 894*, 189−197.
14. Kramer, D. M., and Crofts, A. R. (1995) in *Photosynthesis: from light to biosphere* (Mathis, P., Ed.) pp 575−578, Kluwer Academic Publishers, Dordrecht, The Netherlands.
15. Joliot, P., and Joliot, A. (1986) *Biochim. Biophys. Acta 849*, 211−222.
16. Ding, H., Robertson, D. E., Daldal, F., and Dutton, P. L. (1992) *Biochemistry 31*, 3144−3158.
17. Brandt, U., Schägger, H., and Von Jagow, G. (1988) *Eur. J. Biochem. 173*, 499−506.
18. Xia, D., Yu, C. A., Kim, H., Xian, J. Z., Kachurin, A. M., Zhang, L., Yu, L., and Deisenhofer, J. (1997) *Science 277*, 60−66.
19. Zhang, Z., Huang, L., Shulmeister, V., Chi, Y., Kim, K., Hung, L., Crofts, A., Berry, E., and Kim, S. (1998) *Nature 392*, 677−684.
20. Iwata, S., Lee, J., Okada, K., Lee, J., Iwata, M., Rasmussen, B., Link, T., Ramaswamy, S., and Jap, B. (1998) *Science 281*, 64−71.
21. Kim, H., Xia, D., Yu, C. A., Xia, J. Z., Kachurin, A. M., Zhang, L., Yu, L., and Deisenhofer, J. (1998) *Proc. Natl. Acad. Sci. U.S.A. 95*, 8026−8033.
22. Brugna, M., Albouy, D., and Nitschke, W. (1998) *J. Bacteriol. 180*, 3719−3723.
23. Crofts, A. R., and Berry, E. A. (1998) *Curr. Opin. Struct. Biol. 8*, 501−509.
24. Finazzi, G., Büschlen, S., de Vitry, C., Rappaport, F., Joliot, P., and Wollman, F. (1997) *Biochemistry 36*, 2867−2874.
25. Gorman, D. S., and Levine, R. P. (1965) *Proc. Natl. Acad. Sci. U.S.A. 54*, 1665−1669.
26. Joliot, P., Beal, D., and Frilley, B. (1980) *J. Chim. Phys. 77*, 209−216.
27. Junge, W., and Witt, H. T. (1968) *Z. Naturforsch. 24b*, 1038−1041.
28. Joliot, P., and Delosme, R. (1974) *Biochim. Biophys. Acta 357*, 267−284.
29. Bennoun, P. (1970) *Biochim. Biophys. Acta 216*, 357−363.
30. Finazzi, G., and Rappaport, F. (1998) *Biochemistry 37*, 9999−10005.
31. Delosme, R., Joliot, P., and Trebst, A. (1987) *Biochim. Biophys. Acta 893*, 1−6.
32. Jones, R. W., and Whitmarsh, J. (1988) *Biochim. Biophys. Acta 933*, 258−268.
33. Frank, K., and Trebst, A. (1995) *Photochem. Photobiol. 61*, 2−9.
34. Rich, P., Madgwick, S., and Moss, D. (1991) *Biochim. Biophys. Acta 1058*, 312−328.
35. Degli Esposti, M., de Vries, S., Crimi, M., Ghelli, A., Patarnello, T., and Meyer, A. (1993) *Biochim. Biophys. Acta 1143*, 243−271.
36. Urbach, W., and Kaiser, W. (1972) in *Proceedings of the II International Congress on Photosynthesis Research* (Forti, G., Avron, M., and Melandri, A., Eds) pp 1401−1411, W. Junk N. V. Publishers, The Hague, The Netherlands.
37. Satoh, K., and Fork, D. C. (1983) *Photosynth. Res. 4*, 245−256.
38. Gimmler, H., and Avron, M. (1971) in *Proceedings of the II International Congress on Photosynthesis Research* (Forti, G., Avron, M., and Melandri, A., Eds) pp 789−800, W. Junk N. V. Publishers, The Hague, The Netherlands.
39. Graan, T., and Ort, D. (1986) *Arch. Biochem. Biophys. 248*, 445−451.
40. Williams, J. W., and Morrison, J. (1979) *Methods Enzymol. 63*, 437−467.
41. Sonneveld, A., Rademaker, H., and Duysens, L. N. M. (1980) *Biochim. Biophys. Acta 593*, 272−289.
42. Rich, P. R. (1982) in *Function of quinones in energy conservating systems* (Trumpower, B. L., Ed.) pp 73−83, Academic Press, New York.
43. Fernandez-Velasco, J., and Crofts, A. R. (1991) *Biochem. Soc. Trans. 19*, 588−593.
44. Haehnel, W. (1982) *Biochim. Biophys. Acta 682*, 245−257.
45. Schoepp, B., Brugna, M., Riedel, A., Nitschke, W., and Kramer, D. M. (1999) *FEBS Lett. 450*, 245−250.
46. Rich, P. R., and Bendall, D. S. (1981) in *Vectorial Reaction in Electron and Ion Transport in Mitochondria and Bacteria* (Palmieri, F., Quagliarello, E., Siliprandi, N., and Slater, E. C., Eds.) pp 187−190, Elsevier, Amsterdam.
47. Nanba, M., and Katoh, S. (1986) *Biochim. Biophys. Acta 851*, 484−490.
48. Moser, C. C., Page, C. C., Farid, R., and Dutton, P. L. (1995) *J. Bioenerg. Biomembr. 27*, 263−274.
49. Joliot, P., and Joliot, A. (1988) *Biochim. Biophys. Acta 933*, 319−333.
50. Kuras, R., Wollman, F. A., and Joliot, P. (1995) *Biochemistry 34*, 7468−7475.

BI990424+